Electronic and optical properties of Fe, Pd, and Ti studied by reflection electron energy loss spectroscopy

Tougaard, Sven Mosbæk

Published in:
Journal of Applied Physics

Publication date:
2014

Document version
Submitted manuscript

Citation for pulished version (APA):
Tougaard, S. M. (2014). Electronic and optical properties of Fe, Pd, and Ti studied by reflection electron energy loss spectroscopy. Journal of Applied Physics, 115(243508), [243508].

Electronic and optical properties of Fe, Pd, and Ti studied by reflection electron energy loss spectroscopy

Dahlang Tahir,[1] Jens Kraaer,[2] and Sven Tougaard[2]
[1]*Department of Physics, Hasanuddin University, Makassar 90245, Indonesia*
[2]*Department of Physics, Chemistry, and Pharmacy, University of Southern Denmark, DK-5230 Odense M, Denmark*

(Received 6 May 2014; accepted 18 June 2014; published online 30 June 2014)

We have studied the electronic and optical properties of Fe, Pd, and Ti by reflection electron energy-loss spectroscopy (REELS). REELS spectra recorded for primary energies in the range from 300 eV to 10 keV were corrected for multiple inelastically scattered electrons to determine the effective inelastic-scattering cross section. The dielectric functions and optical properties were determined by comparing the experimental inelastic-electron scattering cross section with a simulated cross section calculated within the semi-classical dielectric response model in which the only input is $\mathrm{Im}(-1/\varepsilon)$ by using the QUEELS-$\varepsilon(k,\omega)$-REELS software package. The complex dielectric functions $\varepsilon(k,\omega)$, in the 0–100 eV energy range, for Fe, Pd, and Ti were determined from the derived $\mathrm{Im}(-1/\varepsilon)$ by Kramers-Kronig transformation and then the refractive index n and extinction coefficient k. The validity of the applied model was previously tested and found to give consistent results when applied to REELS spectra at energies between 300 and 1000 eV taken at widely different experimental geometries. In the present paper, we provide, for the first time, a further test on its validity and find that the model also gives consistent results when applied to REELS spectra in the full range of primary electron energies from 300 eV to 10000 eV. This gives confidence in the validity of the applied method. © *2014 AIP Publishing LLC*. [http://dx.doi.org/10.1063/1.4885876]

I. INTRODUCTION

Electron energy loss spectroscopy (EELS) is a powerful analytical tool for investigating surface modification processes; surface oxidation, corrosion, alloy formation, and quantitative analysis for determination of the optical properties.[1–3] The features in EELS spectra arise from the electron energy losses produced by the excitation of intraband and interband transitions in the solid and from the creation of bulk and surface plasmons.[4–6] The intensities and energy positions of EELS features give information on the joint density of electron states between filled and empty states in the solid. The band gap can be determined by drawing a linear fitted line with maximum negative slope from a point near the onset of energy loss. The crossing point with the zero line determines the band gap value.[7,8] Considering the electronic properties that can be gained from EELS and the fundamental interest in understanding the electronic excitations in solids, comprehensive studies of EELS spectra obtained from different elements are very important.

With the increasing technological importance of nanostructured materials, there is also a growing need for characterization techniques that provide electronic structure information at high spatial resolution. Standard optical techniques do not provide high spatial resolution and special equipment is required for studies at higher photon energies. As a consequence, in recent years, there has been an increasing interest in using valence electron-energy-loss spectroscopy (VEELS) because, in comparison to optical methods, it allows to study a wide energy range and it provides high spatial resolution.[9–11]

VEELS can be done with machines for transmission electron spectroscopy (TEM) with very high lateral resolution but TEM is hard to use for analysis of thin films of a few nanometer thickness. In comparison, reflection electron energy loss spectroscopy (REELS) is well suited for this because, when used at energies of ~1 keV, the inelastic electron mean free path (IMFP) and thereby the probing depth is only on the order of 1–2 nm. Besides this, REELS is experimentally much simpler compared to TEM because no special sample preparation is needed since the experiment can be done directly on the thin film after it is grown on its supporting substrate material. The drawback of REELS compared to TEM is that data interpretation is more involved. This is so because at energies below a few keV, the energy loss processes are strongly influenced by the presence of the surface and in addition, there is a considerable contribution from excitations that take place while the electron is moving in the vacuum above the surface due to interactions between the moving electron and its image charge. Attempts have been done to model REELS spectra by two functions, which correspond to a bulk and a surface term and convolutions of these to model multiple scattering effects.[3,12,13] The validity of this model has been questioned because it was found[12] that inconsistencies resulted when effective cross sections determined from REELS spectra from a wide range of energies were fitted by a linear combination of the surface and bulk energy loss function (ELF). It was further shown that the shape of the energy loss distribution varies in a complex way with the depth where the individual electrons in a REELS experiment are backscattered.[12,14,15] This inspired Yubero, Tougaard, and coworkers to develop a semi-classical dielectric response

model for REELS,[10,14–16] which takes into account the interference between surface and bulk loss processes as well as energy loss that occurs when the moving electron in the vacuum approaches or leaves the surface. It is a one-step model in which the energy loss processes for the full trajectory from the time when the electron leaves the electron gun until the backscattered electron enters the electron spectrometer is calculated and therefore interference effects between surface and bulk excitations are also included.

The Tougaard-Yubero model for REELS[17] which allows to determine the dielectric properties has been successfully used to obtain the electronic and optical properties of several materials, including ultrathin dielectrics, semiconductors, metals and their oxides, transparent oxide films, and polymers.[18–26]

In the present paper, we apply this method to determine the electronic and optical properties of Fe, Pd, and Ti from an analysis of REELS spectra taken at primary energies of 300, 500, 3000, 4000, 6000, and 10 000 eV. We report these properties in terms of the real and imaginary parts of the dielectric function ε, the refractive index n, and the extinction coefficient k of Fe, Pd, and Ti over a wide energy range (0–100 eV).

The validity of the model applied in the present analysis was previously tested and found to give consistent results when applied to REELS spectra at energies between 200 and 2000 eV taken at widely different experimental geometries.[18,27] In the present study, we provide a further test on its validity and find that the model also gives consistent results when applied to REELS spectra taken at all energies in the range of primary electron energies from 0.3 keV to 10 keV for all three metals studied.

II. EXPERIMENT

The REELS spectra were recorded with electron incidence and exit angles of 20° and 15° to the surface normal, respectively, and the hemispherical electron energy analyzer was operated at 20 eV pass energy. The measured spectra were corrected for the energy dependence of the analyzer transmission which is $E^{-0.7}$. The primary-electron energies were 0.3 0.5, 3.0, 4.0, 6.0, and 10.0 keV. The energy resolution, given by the full width at half maximum (FWHM) of the elastic peak of backscattered electrons, was about 0.8 eV, and REELS spectra were measured up to 150 eV energy loss. More information on the experimental details and on the special spectrometer, which was developed to allow REELS to be measured at 10 keV can be found in Ref. 28.

III. DATA ANALYSIS

A. Inelastic-scattering cross sections and ELF

QUEELS-XS-REELS software, which implements the theory by Tougaard and Chorkendorff,[29] was used to remove the multiply scattered electrons from the measured REELS spectra. This method corrects the REELS spectrum for multiple scattered electrons and determines an effective single-scattering cross section $K_{exp}(\hbar\omega)$ times the corresponding inelastic electron mean free path λ, in the form of $\lambda K_{exp}(\hbar\omega)$.

We have used the semi-classical dielectric response model of Yubero and Tougaard,[14,15,17] which has been shown experimentally to be of satisfactory validity[18,27] for the interpretations of the experimental effective cross section in terms of the dielectric function. This model includes interference effects between surface and bulk excitations and excitations that take place after the electron has left the solid and travels in the vacuum. The algorithm is rather complex but it has been implemented in the QUEELS-$\varepsilon(k,\omega)$-REELS software package,[16] which was used in the present work. In this software, all excitations are described by the dielectric function $\varepsilon(k,\omega)$ of the material, a function of wave vector k and frequency ω, which is the only input in the calculations. The dielectric function gives the energy-loss function (ELF) $\mathrm{Im}(-1/\varepsilon)$, which is parameterized as a sum of Drude-Lindhard type oscillators, as described in Refs. 17 and 30

$$\mathrm{Im}\left\{\frac{-1}{\varepsilon(k,\omega)}\right\} = \theta(\hbar\omega - E_g) \times \sum \frac{A_i\gamma_i\hbar\omega}{\left(\hbar^2\omega_{0ik}^2 - \hbar^2\omega^2\right)^2 + \gamma_i^2\hbar^2\omega^2}, \quad (1)$$

where the dispersion relation is given in the form

$$\hbar\omega_{0ik} = \hbar\omega_{0i} + \alpha_i\frac{\hbar^2k^2}{2m}. \quad (2)$$

Here, A_i, γ_i, $\hbar\omega_i$, and α_i are the oscillator strength, damping coefficient, excitation energy, and momentum-dispersion coefficient of the ith oscillator, respectively, and $\hbar k$ is the momentum transferred from the REELS electron to an electron in the solid. The dependence of ω_{0ik} on k is expressed by Eq. (2) with α_i as an adjustable parameter. The step function $\theta(\hbar\omega - E_g)$ is included to describe the effect of the band gap E_g in semiconductors and insulators. Here, $\theta(\hbar\omega - E_g) = 0$ if $\hbar\omega < E_g$ and $\theta(\hbar\omega - E_g) = 1$ if $\hbar\omega > E_g$.

For a given set of oscillators, the theoretical cross section $\lambda K_{th}(\hbar\omega)$ is calculated with the QUEELS-$\varepsilon(k,\omega)$-REELS software and compared to the experimental $\lambda K_{exp}(\hbar\omega)$ inelastic scattering cross section. The parameters A_i, γ_i, $\hbar\omega_i$, and α_i, of the oscillators are varied until good agreement between the calculated and experimental inelastic cross sections is obtained. The oscillator strengths are adjusted to make sure that $\varepsilon(k,\omega)$ fulfills the well-established Kramers-Kronig sum rule,[17,30] which for metals is

$$\frac{2}{\pi}\int_0^\infty \mathrm{Im}\left\{\frac{1}{\varepsilon(k,\omega)}\right\}\frac{d(\hbar\omega)}{\hbar\omega} = 1. \quad (3)$$

B. Optical properties obtained from the energy loss function

The optical properties of materials can be described by the complex dielectric function. Using the parameterization in Eq. (1) allows us to perform an analytical Kramers-Kronig transformation of $\mathrm{Im}\{1/\varepsilon\}$ to obtain the real part $Re\{1/\varepsilon\}$ of the reciprocal of the complex dielectric function.

From $\mathrm{Im}\{1/\varepsilon\}$ and $Re\{1/\varepsilon\}$, we can express the real and imaginary parts of the dielectric function in the form

$$\varepsilon_1 = \frac{\mathrm{Re}\{1/\varepsilon\}}{(\mathrm{Re}\{1/\varepsilon\})^2 + (\mathrm{Im}\{1/\varepsilon\})^2}, \qquad \varepsilon_2 = \frac{\mathrm{Im}\{1/\varepsilon\}}{(\mathrm{Re}\{1/\varepsilon\})^2 + (\mathrm{Im}\{1/\varepsilon\})^2}. \tag{4}$$

The index of refraction n and the extinction coefficient k are given in terms of the dielectric function as follows:[16,30]

$$n = \sqrt{\frac{1}{2}\left(\sqrt{\varepsilon_1^2 + \varepsilon_2^2} + \varepsilon_1\right)}, \quad k = \sqrt{\frac{1}{2}\left(\sqrt{\varepsilon_1^2 + \varepsilon_2^2} - \varepsilon_1\right)}. \tag{5}$$

Tools to perform the Kramers-Kronig transformation and to calculate these optical quantities are also included in the QUEELS-$\varepsilon(\boldsymbol{k},\omega)$-REELS software.[16]

IV. RESULTS AND DISCUSSIONS

The dielectric functions given by the ELF $\mathrm{Im}(-1/\varepsilon)$ (Eq. (1)) were determined by a trial-and-error procedure, in which the parameters of a test ELF function were adjusted until there was satisfactory agreement between the theoretical inelastic cross section $\lambda K_{th}(E_0, \hbar\omega)$ and the experimental inelastic cross section $\lambda K_{exp}(E_0, \hbar\omega)$ for all primary energies considered. The ELF parameters determined in this way are shown in Table I. The dependence of ω_{0ik} on k is generally unknown, but we use Eq. (2) with α_i as an adjustable parameter. The value of α_i is related to the effective electron mass, so that in the present analysis, for oscillators corresponding to the valence electrons in metals we have used $\alpha_i = 1$ and for the more tightly bound core electrons with flat energy bands $\alpha_i = 0.02$. Figure 1 shows a comparison of the experimental inelastic cross sections $\lambda K_{exp}(\hbar\omega)$ (lines) and the theoretical inelastic cross sections λK_{th} $(\hbar\omega)$ (symbol) for Fe, Pd, and Ti. The experimental $\lambda K_{exp}(\hbar\omega)$ inelastic-scattering cross sections were derived from the REELS spectra for Fe, Pd, and Ti at the different primary energies using the QUASES-XS-REELS software.[29]

TABLE I. Parameters used to the model energy loss functions of Pd, Fe, and Ti according to the Drude–Lindhard oscillator theory to give the best fit to the experimental cross section.

	i	$\hbar\omega_{0i}$ (eV)	A_i (eV^2)	γ_i (eV)	α_i
Fe ($E_g = 0$ eV)	1	9.4	13.2	8.0	1.0
	2	16.5	79.5	8.5	1.0
	3	23.6	261.6	10.0	1.0
	4	30.5	33.2	5.8	1.0
	5	56.0	24.2	2.7	0.02
	6	58.0	28.7	3.2	0.02
	7	66.8	138.0	16.0	0.02
	8	92.0	47.4	10.0	0.02
Pd ($E_g = 0$ eV)	1	8.0	8.4	3.7	1.0
	2	10.5	20.9	7.0	1.0
	3	16.8	26.7	6.0	1.0
	4	25.7	208.9	9.8	1.0
	5	33.2	115.2	7.0	1.0
	6	45.0	132.4	19.0	0.02
	7	58.0	130.7	12.7	0.02
	8	69.0	133.4	16.0	0.02
	9	84.0	226.9	35.0	0.02
Ti ($E_g = 0$ eV)	1	9.5	18.9	9.0	1.0
	2	17.6	207.2	5.8	1.0
	3	33.7	3.6	1.2	0.02
	4	45.0	179.5	11.2	0.02
	5	49.8	72.5	6.2	0.02
	6	61.0	1.2	0.5	0.02

Note that for a given material, λK_{th} $(\hbar\omega)$ were calculated for all energies, with the same dielectric function. From the successful fits in Fig. 1, we conclude that the applied model accounts quantitatively well for the variations in the energy loss processes observed in REELS over a very wide range of primary electron energies from 300 eV to 10 keV. This is the first time the validity of the model has been tested for energies up to 10 keV. For very small loss energies (<2 eV), but only at the primary energies 300 eV and 500 eV, there is a deviation between the theoretical inelastic cross section $\lambda K_{th}(E_0, \hbar\omega)$ and the experimental inelastic cross section $\lambda K_{exp}(E_0, \hbar\omega)$ the origin of which is unclear.

It was previously shown[17,18,27] that at low energies, the model also gives a quantitative account for the large variations in the REELS spectra, which are observed when the geometry of the experiment is varied (e.g., for spectra taken at glancing and normal angles of emission). This gives confidence in the validity of the model and thereby in the accuracy of the determined ELFs.

The ELFs for Fe, Pd, and Ti corresponding to the determined ELF parameters shown in Table I are plotted in Figure 2 (left panel) together with the surface energy-loss functions (SELF) $[-1/(\varepsilon + 1)]$, which indicate the positions of surface excitations.[31] In Figure 2 (right panel), we compare our result for Fe, Pd, and Ti to the ELF published by Moreno-Marin *et al.*,[32] Palik,[33] and Werner *et al.*[13] Moreno-Marin *et al.* and Palik determined the ELF by fitting to data from different publications some of which may be subject to surface contamination and this may explain the difference from the present ELF. The data of Werner *et al.* labelled REELS in Fig. 2 were determined from analysis of two REELS spectra from well characterized clean surfaces measured at the primary energies $E_0 = 700$ eV and 3400 eV.[13] This analysis was done using a deconvolution model which involves two functions, a surface and a bulk excitation term and convolutions of these to account for multiple scattering. The relative contribution from the individual multiple scattering terms is calculated from a detailed model for elastic electron scattering of the primary electron as it travels in the surface region. Within the validity of Werner's model, the equations can be solved for the surface and the bulk terms, when REELS spectra taken at two primary energies are used. The dielectric function is determined by a fit to the resulting surface and bulk terms. A possible problem with this model is that the surface term is assumed to be independent of the primary energy and of the angle of electron trajectory to the surface normal, which is unlikely to be true.[14,15] It should also be noted that for the final fitting of the dielectric function the authors use a procedure (Eq. (27) in Ref. 13) in which the statistical weight of the surface term only counts

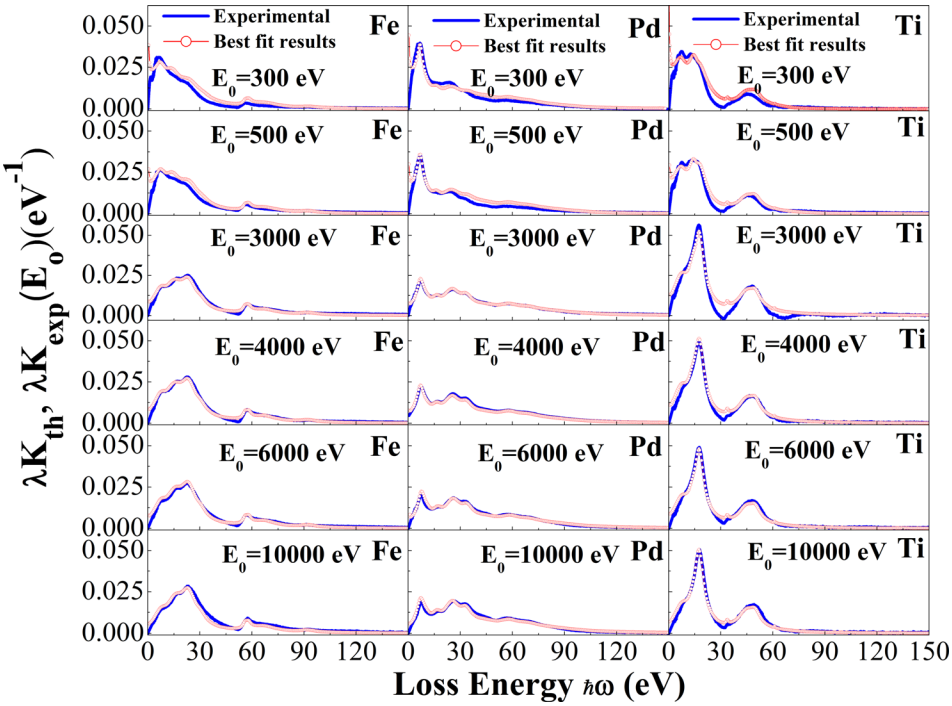

FIG. 1. Experimental inelastic cross sections λK_{exp} for Fe, Pd, and Ti (line) obtained from REELS data compared to the theoretical inelastic cross sections λK_{th} (symbol) calculated with the energy loss function given by the parameters in Table I.

1% and the bulk term counts 99% and that the authors admit that the reason why they have to put such a small emphasis on the reliability of the surface term is due to inaccuracies in their model for the surface term.[13]

Unfortunately, thorough tests of the validity of Werner's model have not been performed yet; for example, the analysis is based on two REELS spectra but it has not been tested whether it provides consistent results when applied to sets of REELS spectra taken at various combinations of geometries and/or combination of energies. On the other hand, it was found[12] that inconsistencies resulted when effective cross sections determined from REELS spectra from a wide range of energies were fitted by a linear combination of the surface and bulk energy loss function. It was further shown that the shape of the energy loss distribution varies in a complex way with the depth where the individual electrons in a REELS experiment are backscattered[14,15] and with angle of emission and this also point to the conclusion that an analysis of

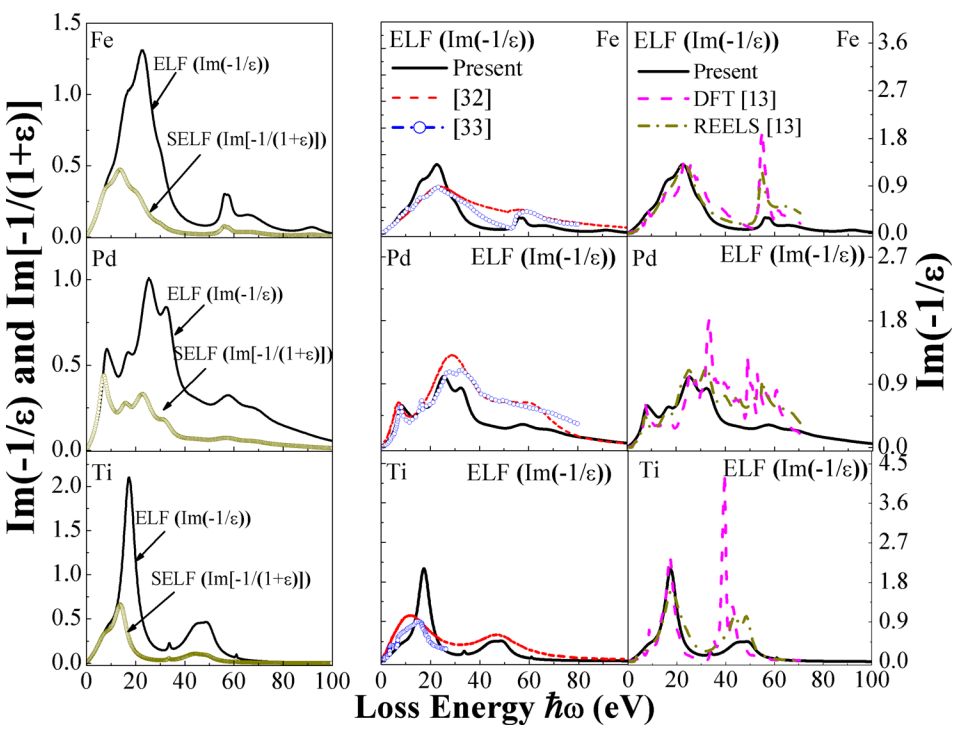

FIG. 2. Energy loss functions (ELF) and surface energy loss function (SELF) for Fe, Pd, and Ti. ELF in comparison with results from Moreno-Marin *et al.*,[32] Palik,[33] and Werner *et al.*[13]

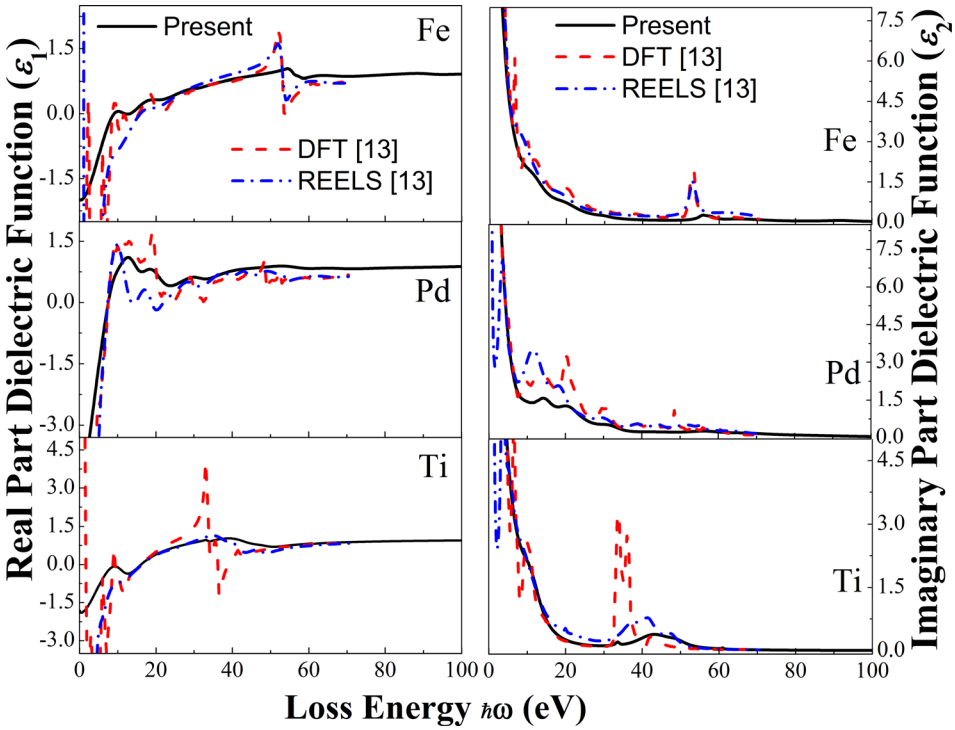

FIG. 3. The real part ε_1 and imaginary part ε_2 of the dielectric functions. Also shown are the results by Werner *et al.* from DFT calculations and his analysis of REELS taken at 700 eV and 3400 eV.[13]

REELS at low primary energies, expressed in terms of just two fixed functions, a bulk and a surface excitation function, is insufficient for a quantitative description.

In contrast to this, the model we have applied in this paper has been shown to give a consistent dielectric function when applied to REELS taken at a wide range of energies and a wide range of geometries.

For these reasons, we ascribe the differences between the present results and those based on the REELS analysis in Ref. 13 to differences in the applied theoretical models. As seen in Fig. 2 (far right panel), there is a fair agreement between the present results and REELS[13] in the region below ~50 eV for Fe and below 30 eV for Pd and Ti but there are very large differences at higher energies.

We have no experience with the code and the model used for the density functional theory (DFT) calculations in Ref. 13 and can therefore not comment on the accuracy of these results.

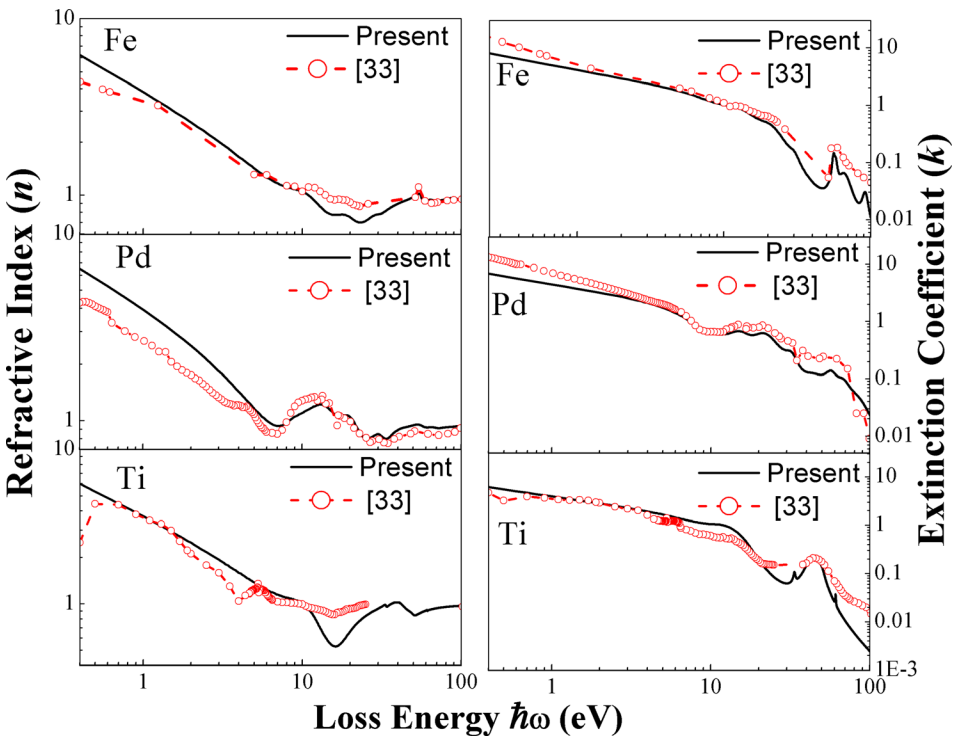

FIG. 4. The refractive index n and extinction coefficient k of Fe, Pd, and Ti. Also shown are Palik's compiled optical data.[33]

The ELF determined for Pd has 9 oscillators, for Fe 8 oscillators, and for Ti 6 oscillators. The oscillators for Pd are at 8, 10.5, 16.8, 25.7, 33.2, 45, 58, 69, and 84 eV, for Fe at 9.4, 16.5, 23.6, 30.5, 56, 58, 66.8, and 92 eV, and for Ti at 9.5, 17.6, 33.7, 45, 49.8, and 61 eV.

The main peak as indicated by the strength A_i of the oscillators of the ELF in Fig. 2 is 23.6 eV for Fe, 25.7 eV for Pd, and 17.6 eV for Ti (see Table I and Figure 2). Figure 2 shows that the ELF can be used to clearly distinguish between Fe, Pd, and Ti.

In Ref. 25, oscillators were reported for Cu and an oscillator at ~10 eV was ascribed to excitation of electrons 3 eV below E_F to states ~7.4 eV above E_F. A similar oscillator is present at 10.5 eV for Pd, 9.4 eV for Fe, and 9.5 eV for Ti. For Pd, the first oscillator at 8.0 eV may correspond to excitation of *d* electrons from ~2 eV below E_F to states ~5.5 eV above E_F, which is similar to the oscillator for Cu at 7.1 eV as reported in Ref. 25. The narrow oscillators for Fe at 56 eV and 58 eV correspond to excitation of Fe 3p electrons with binding energy 53 eV to unoccupied states above E_F and the peak at 92 eV to excitation of Fe 3s electrons (binding energy 92 eV). Similarly, the oscillator for Pd at 58 eV corresponds to excitation of Pd 4p electrons (binding energy 52 eV) and for Ti the oscillators at 33.7 eV and 61 eV correspond to excitation of Ti 3p and Ti 3s electrons (binding energies 33 eV and 59 eV, respectively). All binding energy values are taken from Ref. 34.

The optical properties of Fe, Pd, and Ti were determined from the ELF as described in Sec. III. Figure 3 shows the real part ε_1 and the imaginary part ε_2 of the dielectric functions as well as the refractive index *n* and the extinction coefficient *k*. As can be seen in Fig. 3, the intensities, the energy-loss positions, and the shapes of the dielectric function (ε_1 and ε_2) for Fe, Pd, and Ti are different.

In the energy-loss region above the bulk plasmon peak, the transparency of Fe, Pd, and Ti is higher.[30] This result is consistent with the fact that, in this energy-loss region, ε_2 and *k* go to zero as can be seen clearly in Figure 3.

Figure 4 shows the refractive index *n* and extinction coefficient *k* as a function of energy-loss for Fe, Pd, and Ti (present work) together with corresponding data from Palik's handbook of optical data.[33] For Fe, Pd, and Ti, the presently determined *n* and *k* show peaks in reasonably good agreement with Palik's compiled data. For Ti, Palik's data for *n* are available only at energy loss <25 eV. From our results, we conclude that the intensities, shapes, and peak positions of the dielectric function (ε_1 and ε_2), refractive index (*n*), and extinction coefficient (*k*) are very different for Fe, Pd, and Ti.

V. CONCLUSION

In this work, we determined electronic and optical properties of Fe, Pd, and Ti by quantitative analysis of REELS data. The REELS data were corrected for multiple inelastically scattered electrons to determine the effective inelastic scattering cross section $K_{exp}(\hbar\omega)$ times the corresponding inelastic mean free path λ, in the form of λK_{exp}. The energy-loss functions of Fe, Pd, and Ti were obtained by comparing this experimental cross-section with a theoretical λK_{th} cross section calculated within the semi-classical dielectric response model in which the only input is $\mathrm{Im}(-1/\varepsilon)$. This model is implemented in the QUEELS-$\varepsilon(k,\omega)$-REELS software package which was used here. This was done for REELS spectra, recorded for primary energies of 300, 500, 3000, 4000, 6000, and 10 000 eV. For all three metals, it was found that the same $\mathrm{Im}(-1/\varepsilon)$ gave good agreement for all energies. It was previously shown that the model also gives consistent $\mathrm{Im}(-1/\varepsilon)$ from analysis of REELS taken in several geometries corresponding to, e.g., glancing and normal emission. This agreement gives confidence in the validity of the model and in the determined $\mathrm{Im}(-1/\varepsilon)$. By Kramers–Kronig transformation of the determined $\mathrm{Im}(-1/\varepsilon)$, the real and imaginary parts (ε_1 and ε_2) of the dielectric function, and the refractive index *n* and extinction coefficient *k* were determined for Fe, Pd, and Ti in the 0–100 eV energy range. It is found that the ELFs are quite different and that the experimental ELF can be used to clearly distinguish between Fe, Pd, and Ti.

ACKNOWLEDGMENTS

We thank the Hasanuddin University, Indonesia by BOPTN 2014 program for financial support.

[1]S. Tougaard, Surf. Interface Anal. **26**, 249 (1998).
[2]Kh. Zakeri, Y. Zhang, and J. Kirschner, J. Electron Spectrosc. Relat. Phenom. **189**, 157–163 (2013).
[3]W. S. M. Werner, Phys. Rev. B **74**, 075421 (2006).
[4]Z. H. Zhang, H. L. Tao, L. L. Pan, L. Giu, M. He, B. Song, and Q. Li, Scr. Mater. **69**, 262–265 (2013).
[5]T. Nagatomi, Y. Takai, B. V. Crist, K. Goto, and R. Shimizu, Surf. Interface Anal. **35**, 174–178 (2003).
[6]T. Nagatomi and K. Goto, Phys. Rev. B **75**, 235424 (2007).
[7]D. Tahir, E. K. Lee, S. K. Oh, T. T. Tham, H. J. Kang, H. Jin, S. Heo, J. C. Park, J. G. Chung, and J. C. Lee, Appl. Phys. Lett. **94**, 212902 (2009).
[8]H. Jin, S. K. Oh, H. J. Kang, S. W. Lee, Y. S. Lee, and M. H. Cho, Appl. Phys. Lett. **87**, 212902 (2005).
[9]R. Erni and N. D. Browning, Ultramicroscopy **104**, 176 (2005).
[10]P. L. Potapov, H.-J. Engelmann, E. Zschech, and M. Stöger-Pollach, Micron **40**, 262 (2009).
[11]M. R. S. Huang, R. Erni, H.-Y. Lin, R.-C. Wang, and C.-P. Liu, Phys. Rev. B **84**, 155203 (2011).
[12]F. Yubero and S. Tougaard, Surf. Interface Anal. **19**, 269 (1992).
[13]W. S. M. Werner, K. Glantsching, and C. A. Draxl, J. Phys. Chem. Ref. Data **38**, 1013 (2009).
[14]F. Yubero and S. Tougaard, Phys. Rev. B **46**, 2486 (1992).
[15]F. Yubero, J. M. Sanz, B. Ramskov, and S. Tougaard, Phys. Rev. B **53**, 9719 (1996).
[16]S. Tougaard and F. Yubero, see http://www.quases.com for "QUEELS-ε(k,ω)-REELS: Software package for quantitative analysis of electron energy loss spectra; dielectric function determined by reflection electron energy loss spectroscopy," Version 3.02, 2008.
[17]S. Tougaard and F. Yubero, Surf. Interface Anal. **36**, 824 (2004).
[18]S. Hajati, O. Romanyuk, J. Zemek, and S. Tougaard, Phys. Rev. B **77**, 155403 (2008).
[19]D. Tahir, E. K. Lee, S. K. Oh, H. J. Kang, S. Heo, J. G. Chung, J. C. Lee, and S. Tougaard, J. Appl. Phys. **106**, 084108 (2009).
[20]D. Tahir, E. K. Lee, E. H. Choi, S. K. Oh, H. J. Kang, S. Heo, J. G. Chung, J. C. Lee, and S. Tougaard, J. Phys. D: Appl. Phys. **43**, 255301 (2010).
[21]O. Romanyuk, P. Jiricek, J. Zemek, S. Tougaard, and T. Paskova, J. Appl. Phys. **110**, 043507 (2011).
[22]D. Tahir, Y. J. Cho, S. K. Oh, H. J. Kang, H. Jin, S. Heo, J. G. Park, J. C. Lee, and S. Tougaard, Surf. Interface Anal. **42**, 1566–1569 (2010).
[23]D. Tahir, E. K. Lee, S. K. Oh, H. J. Kang, E. H. Lee, J. G. Chung, J. C. Lee, and S. Tougaard, Surf. Interface Anal. **42**, 906–910 (2010).
[24]D. Tahir and S. Tougaard, J. Appl. Phys. **111**, 054101 (2012).

[25]D. Tahir and S. Tougaard, J. Phys.: Condens. Matter **24**, 175002 (2012).
[26]H. C. Shin, D. Tahir, S. Seo, Y. R. Denny, S. K. Oh, H. J. Kang, S. Heo, J. G. Chung, J. C. Lee, and S. Tougaard, Surf. Interface Anal. **44**, 623–627 (2012).
[27]F. Yubero, D. Fujita, B. Ramskov, and S. Tougaard, Phys. Rev. B **53**, 9728 (1996).
[28]S. Tougaard and J. Kraaer, Phys. Rev. B **43**, 1651 (1991).
[29]S. Tougaard and I. Chorkendorff, Phys. Rev. B **35**, 6570 (1987); See http://www.quases.com for information about QUASES-XS-REELS software.
[30]F. Wooten, *Optical Properties of Solid* (Academic Press, New York, 1972).
[31]G. L. Tan, L. K. DeNoyer, R. H. French, M. J. Guittet, and M. G. Soyer, J. Electron Spectrosc. Relat. Phenom. **142**, 97 (2005).
[32]J. C. Moreno-Marin, I. Abril, S. H. Avalos, and R. G. Molina, Nucl. Instrum. Methods Phys. Res., Sect. B **249**, 29–33 (2006).
[33]E. D. Palik, *Handbook of Optical Constants of Solids* (Academic Press, New York, 1985).
[34]*Surface Analysis by Auger and X-Ray Photoelectron Spectroscopy*, edited by D. Briggs and J. T. Grant (IM-Publications, Chicester, 2003).